Technical Report No. 145

AXISYMMETRICAL CREEP BUCKLING OF CLAMPED SHALLOW SPHERICAL SHELLS

N. C. Huang

Division of
ENGINEERING
MECHANICS

STANFORD
UNIVERSITY

December 1963

Prepared under
Office of Naval Research
Contract Nonr 225(69)
Contract Report No. 2

AXISYMMETRICAL CREEP BUCKLING OF CLAMPED SHALLOW SPHERICAL SHELLS*

N. C. Huang
Stanford University

Introduction

The problem of axisymmetrical buckling of clamped shallow spherical elastic shells under uniform external pressure (Figure 1) has been studied by many authors [1-4]** with different numerical methods. Consistent results for the buckling pressure for shells with a large range of geometrical parameters were obtained in their work. In this paper we shall consider the effect of viscoelastic properties of shells on the axisymmetrical buckling. For viscoelastic shells under constant uniform pressure, the average vertical deflection increases with time as shown in Figure 2. When time reaches a critical value t_{cr}, the rate of increase of the average vertical deflection becomes very high, which indicates the initiation of snapping of the shell at this instant. After snapping,

---

* The results in this paper were obtained under Contract Nonr 225(69) by Stanford University with the Office of Naval Research, Washington, D. C. Reproduction in whole or in part is permitted for any purpose of the United States Government.

** Numbers in the raised square brackets designate References at the end of this paper.

the shell continues to deform as shown in Figure 2. Our interest is to find the critical time t_{cr} for different pressures and for shells with different geometrical parameters. The pressure on shells is considered to be applied either by pressurized air in a chamber of large volume or by an incompressible fluid. For the latter loading condition, the average deflection remains constant and the applied pressure relaxes. In this paper, the relaxation of external pressure of this type is analyzed, as well as prescribed pressure increases.

Basic Equations

Consider an elastic clamped shallow spherical shell as shown in Figure 1. For axisymmetrical deformation, the governing differential equations and boundary conditions are found in [1] as

$$\frac{E\,h^3}{12(1-\nu^2)}\left[r\,\frac{d}{dr}\left(r\,\frac{d\beta}{dr}\right)-\beta\right]+\frac{2H}{a^2}\,r^2\psi=-\frac{1}{2}q\,r^3+r\psi\beta \qquad (1)$$

$$\frac{1}{h}\left[r\,\frac{d}{dr}\left(r\,\frac{d}{dr}\right)-\psi\right]-\frac{2EH}{a^2}\,r^2\,\beta=-\frac{E}{2}\,r\,\beta^2 \qquad (2)$$

$$\beta=0 \qquad \text{at} \quad r=a \qquad (3)$$

$$a\,\frac{d\psi}{dr}-\nu\psi=0 \qquad \text{at} \quad r=a \qquad (4)$$

where $\beta = -\frac{dw}{dr}$, w is the vertical deflection of the shell, ψ is a stress function, and E and ν are the Young's modulus and Poisson's ratio respectively. Let E_o and ν_o be two constants and put

$$I_1 = \frac{E}{E_o}$$

$$I_2 = \frac{1-\nu_o^2}{1-\nu^2} \; I_1$$

$$\lambda = 2\,[3(1-\nu_o^2)]^{\frac{1}{4}} \left(\frac{H}{h}\right)^{\frac{1}{2}}$$

$$x = \frac{\lambda r}{a}$$

$$\theta = \frac{\lambda a}{2H}\,\beta$$

$$\Phi = \frac{12(1-\nu_o^2)a}{\lambda E_o h^3}\,\psi$$

$$q_o = \frac{32 E_o H^3 h}{\lambda^2 a^4}$$

$$p = \frac{q}{q_o}$$

Equations (1-4) can then be written as

$$I_2(x^2\theta'' + x\,\theta' - \theta) = -x^2\Phi - 2px^3 + x\,\theta\,\Phi \qquad (5)$$

$$x\,\Phi'' + x\,\Phi' - \Phi = I_1\,(x^2\theta - \tfrac{1}{2}\,x\theta^2) \qquad (6)$$

$$\theta(\lambda) = 0 \tag{7}$$

$$\lambda\Phi'(\lambda) - \nu\,\Phi(\lambda) = 0 \tag{8}$$

where $(\ )' \equiv \frac{d}{dx}(\ )$. The material properties are involved in the constants I_1 and I_2.

In our viscoelastic theory, we use the following assumptions: (1) the strain components in the shell are small so the constitutive equations are linear; (2) for mathematical convenience, the bulk modulus of the shell, K, is assumed to be independent of time; (3) the Kirchhoff's hypotheses hold in the whole process of deformation; (4) the shell is assumed to deform quasi-statically, i.e. the effect due to its inertia force is neglected.

In the viscoelastic problem, the Young's modulus E is replaced by an integral operator with a kernal function E(t). The kernal function equivalent to Poisson's ratio in elastic case, $\nu(t)$, can be found directly from the relation

$$\nu(t) = \frac{1}{2} - \frac{E(t)}{6K} \tag{9}$$

We use the notation $E_o = E(0)$ and $\nu_o = \nu(0)$, then q_o defined above is the classical buckling pressure of a complete spherical shell with the same thickness and radius of curvature. The constants I_1 and I_2 are replaced by the integral operators, with kernal functions $I_1(t)$ and $I_2(t)$ which are determined by the following equations:

$$I_1(t) = \frac{E(t)}{E_o} \tag{10}$$

$$(1-\nu) * (1+\nu) * I_2 = (1-\nu_o^2)\, I_1 \tag{11}$$

where the starred notation represents the integral operation as shown in the following example:

$$I * f = \int_{-\infty}^{t} I(t-\tau)\, \frac{df}{d\tau}\, d\tau$$

Thus, equation (11) is a Volterra integral equation for I_2. Examining the derivation of equations (1-4) in [1], we are able to derive the governing equations for the deformation of viscoelastic shells under the above assumptions by applying the correspondence principle to equations (5-8):

$$I_2^* (x^2\theta'' + x\theta' - \theta) = - x^2\Phi - 2px^3 + x\theta\Phi \tag{12}$$

$$x\Phi'' + x\Phi' - \Phi = I_1 * (x^2\theta - \tfrac{1}{2} x\theta^2) \tag{13}$$

$$\theta(\lambda) = 0 \tag{14}$$

$$\lambda\Phi'(\lambda) - \nu * \Phi(\lambda) = 0 \tag{15}$$

where θ, Φ and p are time dependent and $(\ )' \equiv \frac{\partial}{\partial x}(\ )$. Equations (12) and (13) are two nonlinear integro-differential equations for the two unknown functions $\theta(x,t)$ and $\Phi(x,t)$. These equations will be solved numerically. The average vertical deflection ρ is found in [1] as

$$\rho = \frac{1}{\lambda^2} \int_0^\lambda x^2 \theta \, dx \tag{16}$$

Let M_r and M_t be the meridional and circumferential moments respectively. Put

$$m_r = \frac{6(1-\nu_o^2)}{E_o h^3} \frac{a^2}{H} M_r \tag{17}$$

$$m_t = \frac{6(1-\nu_o^2)}{E_o h^3} \frac{a^2}{H} M_r \tag{18}$$

From the stress strain relations, we have

$$m_r = I_2 * \theta' - I_3 * (\frac{\theta}{x}) \tag{19}$$

$$m_t = I_2 * (\frac{\theta}{x}) - I_3 * \theta' \tag{20}$$

where the operator I_3 is defined as

$$I_3 = I_2 * \nu \tag{21}$$

Hence, M_r and M_t can be obtained from θ by numerical differentiation and integrations.

Numerical Method

The viscoelastic material in our investigation is polymethylmethacrylate. The nondimensional relaxation modulus is found in [5] as

$$I_1(t) = 10^{-1.5}\{1 + \mathrm{erf}[0.31(\log_{10} t - 3.6)]\} \qquad (22)$$

we take $\nu_o = 0.35$ which is equivalent to $K/E_o = 1.111$. Let $t = t_n$. We shall use the following approximation as shown in [6] for the time integration:

$$I*f = I(0)f_n - \frac{1}{2}\sum_{j=1}^{n-1}\{(f_{j+1} + f_j)[I(t_n - t_{j+1}) - I(t_n - t_j)]\}$$

$$= \frac{1}{2}[f_n\, G(I, t_n) - F(I, f_n)] \qquad (23)$$

where $F(I, f_n) = f_{n-1}[I(0) - I(t_n - t_{n-1})]$

$$+ \sum_{j=1}^{n-2}\{(f_{j+1} + f_j)[I(t_n - t_{j+1}) - I(t_n - t_j)]\} \qquad (24)$$

$$G(I, t_n) = I(0) + I(t_n - t_{n-1}) \qquad (25)$$

From the above definition, $F(I, f_n)$ is linear with respect to f_n, i.e.

$$F(I, f_n+g_n) = F(I, f_n) + F(I, g_n)$$

$$F(I, kf_n) = kF(I, f_n) \quad \text{for constant } k.$$

Let $(1-\nu) * \bar{I}_2 = I_1$

From equation (11)

$$(1+\nu) * I_2 = (1-\nu_o^2)\bar{I}_2$$

Using equation (23), we obtain

$$(\bar{I}_2)_n = \frac{2(I_1)_n + F[1-\nu, (\bar{I}_2)_n]}{G(1-\nu, t_n)} \tag{26}$$

$$(I_2)_n = (1-\nu_o^2)\, \frac{2(\bar{I}_2)_n + F[1+\nu, (I_2)_n]}{G(1+\nu, t_n)} \tag{27}$$

where the subscript n designates the values at $t = t_n$. Hence, $I_2(t)$ can be evaluated numerically. Let

$\Delta x = \frac{\lambda}{m}$, where m is the total number of equal space steps. Define

$$x_i = (i-1)\Delta x$$

$$p_j = p(t_j)$$

$$\theta_{ij} = \theta(x_i, t_j) \qquad \text{and} \qquad \Phi_{ij} = \Phi(x_i, t_j)$$

The first and second partial derivatives of θ with respect to x can be approximated by the central difference formulae:

$$\theta'_{ij} = \frac{1}{2\Delta x}\left(-\theta_{i-1,j} + \theta_{i+1,j}\right)$$

$$\theta''_{ij} = \frac{1}{(\Delta x)^2}\left(\theta_{i-1,j} - 2\theta_{ij} + \theta_{i+1,j}\right)$$

Equations (12)-(15) can be written as the following matrix difference equations:

$$A_{in}y_{i-1,n} + B_{in}y_{in} + C_{in}y_{i+1,n} = D_{in} \tag{28}$$

$$E_n y_{mn} + F_n y_{m+1,n} + G_n y_{m+2,n} = H_n \tag{29}$$

where

$$y_{in} = \begin{bmatrix} \theta_{in} \\ \Phi_{in} \end{bmatrix} \tag{30}$$

$$A_{in} = \begin{bmatrix} \left[(i-1)^2 - \frac{i-1}{2}\right]G(I_2, t_n) & 0 \\ 0 & (i-1)^2 - \frac{i-1}{2} \end{bmatrix} \tag{31}$$

$$B_{in} = \begin{bmatrix} -[2(i-1)^2+1]G(I_2, t_n) & 2x_i^2 \\ -\frac{1}{2}x_i^2\, 6(I_1, t_n) & -[2(i-1)^2+1] \end{bmatrix} \tag{32}$$

$$C_{in} = \begin{bmatrix} [(i-1)^2 + \frac{i-1}{2}]G(I_2, t_n) & 0 \\ 0 & (i-1)^2 + \frac{i-1}{2} \end{bmatrix} \quad (33)$$

$$D_{in} = \begin{bmatrix} s_{in} \\ t_{in} \end{bmatrix} \quad (34)$$

$$E_n = \begin{bmatrix} 0 & 0 \\ 0 & 1 \end{bmatrix} \quad (35)$$

$$F_n = \begin{bmatrix} 1 & 0 \\ 0 & \frac{1}{m+1} G(\nu, t_n) \end{bmatrix} \quad (36)$$

$$G_n = \begin{bmatrix} 0 & 0 \\ 0 & -1 \end{bmatrix} \quad (37)$$

$$H_n = \begin{bmatrix} 0 \\ \frac{1}{m+1} F(\nu, \Phi_{m+1,n}) \end{bmatrix} \quad (38)$$

$$S_{in} = [(i-1)^2 - \frac{i-1}{2}]F(I_2, \theta_{i-1,n}) - [2(i-1)^2+1]F(I_2, \theta_{in})$$
$$+[(i-1)^2 + \frac{i-1}{2}]F(I_2, \theta_{i+1,n}) - 4p_n x_i^3 + 2x_i \theta_{in} \Phi_{in} \quad (39)$$

$$T_{in} = -\frac{1}{4} x_i \theta_{in} G(I_1, t_n) - \frac{1}{2} x_i^2 F(I_1, \theta_{in}) + \frac{1}{4} F(I_1, \theta^2_{in}) \quad (40)$$

In our numerical analysis, one extra space station at $x = \lambda + \Delta x$ is added for the convenience of representation. Equations (39) and (40) contain terms nonlinear in θ_{in} and Φ_{in}. An interative method is used to solve this non-linear problem, i.e. we assume the values for θ_{in} and Φ_{in} and evaluate θ_{in} and Φ_{in} by taking s_{in} and T_{in} as known functions. Such iterations continue until a certain convergence criterion is satisfied. If D_{in} is known, we evaluate y_{in} by the numerical technique given in [7]. Let

$$y_{in} = P_{in}\, y_{i+1,n} + Q_{in} \quad (41)$$

where P_{in} is a two-by-two matrix and Q_{in} is a column vector.

From equation (28), we have

$$(A_{in}P_{i-1,n}+B_{in})\, y_{in} + C_{in}\, y_{i+1,n} = D_{in} - A_{in}\, Q_{i-1,n}$$

Therefore,

$$P_{in} = -L_{in}C_{in} \quad (42)$$

$$Q_{in} = L_{in}(D_{in}-A_{in}Q_{i-1,n}) \quad (43)$$

where

$$L_{in} = (A_{in}P_{i-1,n} + B_{in})^{-1} \quad (44)$$

Since $y_{1n} = 0$

$$P_{1n} = Q_{1n} = 0 \tag{45}$$

Equations (42) and (43) are the recurrence formulae for P_{in} and Q_{in}, Therefore, the value of P_{in} and Q_{in} can be determined for $i = 1,2,\ldots m+1$. Substituting equation (41) into equation (29) we can show that

$$y_{m+2,n} = (R_n P_{m+1,n} + G_n)^{-1}(H_n - E_n Q_{mn} - R_n Q_{m+1,n}) \tag{46}$$

where

$$R_n = E_n P_{mn} + F_n \tag{47}$$

After $y_{m+2,n}$ is determined by equations (46), $y_{in}(i=1,2,\ldots m+1)$ and ρ can be evaluated by equations (41) and (16) respectively.

In the case where ρ is prescribed as a constant, it is found by the following procedure that the external pressure relaxes. Multiplying both sides of equation (12) by dx and integrating from $x = 0$ to $x = \lambda$, we have

$$\lambda^2 I_2 * \theta'(\lambda) = -\frac{p}{2}\lambda^4 + \int_0^\lambda x\Phi(\theta - x)dx \tag{48}$$

Again, if we multiply both sides of equation (12) by x^2dx and integrate, we obtain

$$I_2 * [\lambda^2\theta'(\lambda) + 8\rho] = -\frac{p}{3}\lambda^4 + \frac{1}{\lambda^2}\int_0^\lambda x^3\Phi(\theta - x)\,dx \tag{49}$$

Eliminating $I_2 * \theta'(\lambda)$ from equations (48) and (49) and solving for p, we have

$$p = \frac{6}{\lambda^4} \left[8\rho I_2 + \int_0^\lambda x(1+\frac{x}{\lambda})(1-\frac{x}{\lambda})\, \Phi(\theta-x)dx\right] \tag{50}$$

hence, the relaxing external pressure at any time can be determined.

In our numerical calculation, we computed $I_1(t)$, $I_2(t)$, $I_3(t)$ and $v(t)$ by equations (22), (27), (21) and (9) respectively. These values are plotted as functions of t in Figure 3. The functions θ and Φ were evaluated by iterative procedure from equations (39), (40) (41), (46), etc. If p was prescribed, the calculation continued until the absolute value of the difference between the value of ρ and the average value of ρ's found in the five previous iterative processes was less than 0.001. If ρ was prescribed, the convergence criterion used here was that the absolute value of the difference between the value of p calculated by equation (50) and the average value of p's found in the five previous interative processes was less than 0.001. In our computation, we used a log time step, therefore, the variations of θ and Φ at very early times could be taken into consideration. The calculated values of θ and Φ at each time step were stored for the sake of the history dependence of the function F [equation (24)]. For the purpose of comparison, numerical calculations were carried out for $\lambda = 6$ and $p = 0.8$ (i.e. 80% of the classical buckling pressure of a complete sphere) for different time intervals and space intervals. The results are shown in Figure 4. Although there are discrepancies between these curves for the

different space intervals used, the critical times obtained from these curves show no noticeable difference. We, therefore, used $\Delta x = 0.125$ and $\Delta(\log_{10} t) = 0.5$ in the subsequent computations.

When t approaches t_{cr}, ρ increases very rapidly. The iterative process becomes divergent as t exceeds a certain value t_{cr}. This divergence of our iterative procedure arises from the fact that there does not exist a equilibrium state in the neighbourhood of the equilibrium state just before buckling defined by positive increaments of time. We define t_{cr} such that at $t = t_{cr}$, the iterative process converges and at $t = 10^{\log_{10} t_{cr} + 0.005} = 1.012\, t_{cr}$, the iterative process diverges. The maximum relative error of t_{cr} found from this definition is less than 1.2%.

Numerical Results and Discussions

A program for numerical computations was written in the BALGOL machine language and all calculations were made on the IBM 7090 digital computer at Stanford University Computation Center. These facilities were in part made available under the National Science Foundation Grant NSF-GP 948. The average vertical deflection under different pressures are plotted against time for $\lambda = 6$ and $\lambda = 7$ in Figures 5 and 6. The critical times under different pressures are shown in Table 1 and Figure 7.

From Figure 7, we find that the critical time decreases when the pressure increases. The rate of decrease becomes very rapid when the pressure is close to the elastic buckling pressure. As we know, the critical time is zero when the external pressure reaches the elastic buckling pressure based

on the moduli for instantaneous loading. Since the elastic buckling pressure for $\lambda = 7$ is higher than that for $\lambda = 6$[1], under the same external pressure, the shell with $\lambda = 7$ possesses longer critical time than the shell with $\lambda = 6$. Figures 8, 9 and 10 show the distributions of θ, m_r and m_t at different times for $\lambda = 6$ and $p = 0.85$. The θ curves in Figure 8 are the slope distributions before buckling. After buckling, the values of θ are presumably positive in the whole range of x. Before buckling, the vertical deflection grows with time but the shape of the deflection curve remains approximately the same. From Figures 9 and 10, we find that the moments near the shell edge relax and that the moments in the region outside the boundary layer grow with time as a result of magnification of the slope curve (Figure 8).

The case in which $\rho = 1.092$ was evaluated and the corresponding relaxation curve of external pressure p is shown in Figure 11 for $\lambda = 6$. Figures 12, 13 and 14 represent the distribution of θ, m_r and m_t at different time stages. When time increases, the deflections in the central portion of the shell decrease but the deflections elsewhere increase so the average vertical deflection remains a constant. In Figure 13 and 14, moments decrease with increasing time because of relaxation of external pressure.

Acknowledgement

The author is grateful to Professor E. H. Lee and Dr. E. Appleby for their generous assistance in the reading of proof and for valuable suggestions.

REFERENCES

[1] Budiansky, B., "Buckling of Clamped Shallow Spherical Shells," Proceedings of the Symposium on the Theory of Thin Elastic Shells, Delft, August 1959, North Holland Publishing Company, Amsterdam, p. 64.

[2] Weinitschke, H., "On the Stability Problem for Shallow Spherical Shells," Journal of Mathematics and Physics. Vol. 38, No. 4, p. 209, January 1960.

[3] Thurston, G. A., "A Numerical Solution of the Nonlinear Equations for Axisymmetric Bending of Shallow Spherical Shells," Journal of Applied Mechanics, Vol. 28, No. 4, p. 557, December 1961.

[4] Archer, R. R., "On the Numerical Solution of the Nonlinear Equations for Shells of Revolution," Journal of Mathematics and Physics, Vol. 4, No. 3, p. 165, September 1962.

[5] Bischoff, J., Catsiff, E. and Tobolsky, A. V., "Elastoviscous Properties of Amosphous Polymers in the Transition Region—I," Journal of the American Chemical Society, Vol. 74, p. 3378, 1952.

[6] Lee, E. H. and Rogers, T. G., "Solution of Viscoelastic Stress Analysis Problems Using Measured Creep or Relaxation Functions," Journal of Applied Mechanics, Vol. 30, No. 1, p. 127, March 1963.

[7] Ralston, A. and Wilf, H., "Mathematical Methods for Digital Computers," Wiley and Sons, p. 121, 1960.

[8] Gurtin, M. E. and Sternberg, E., "On the Linear Theory of Viscoelasticity," Archive for Rational Mechanics and Analysis Vol. 11, p. 291, 1962.

	$\log_{10}(t_{cr})$	
P	$\lambda = 6$	$\lambda = 7$
0.80	-0.22	0.14
0.85	-0.59	-0.17
0.90	-1.05	-0.48
0.95	-1.75	-0.91

Table 1

Critical Times for $\lambda = 6$ and $\lambda = 7$

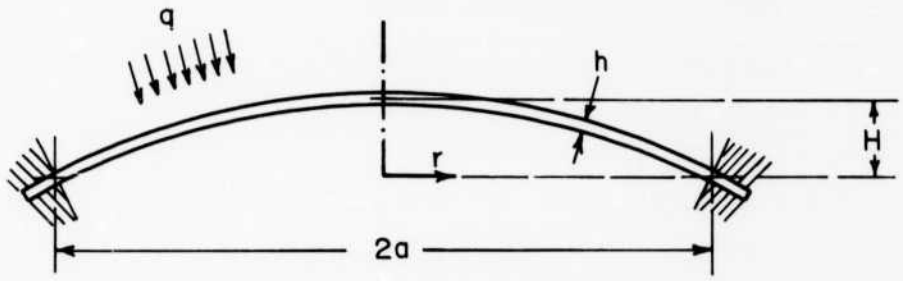

FIG. 1. Geometry of Clamped Shallow Spherical Shells

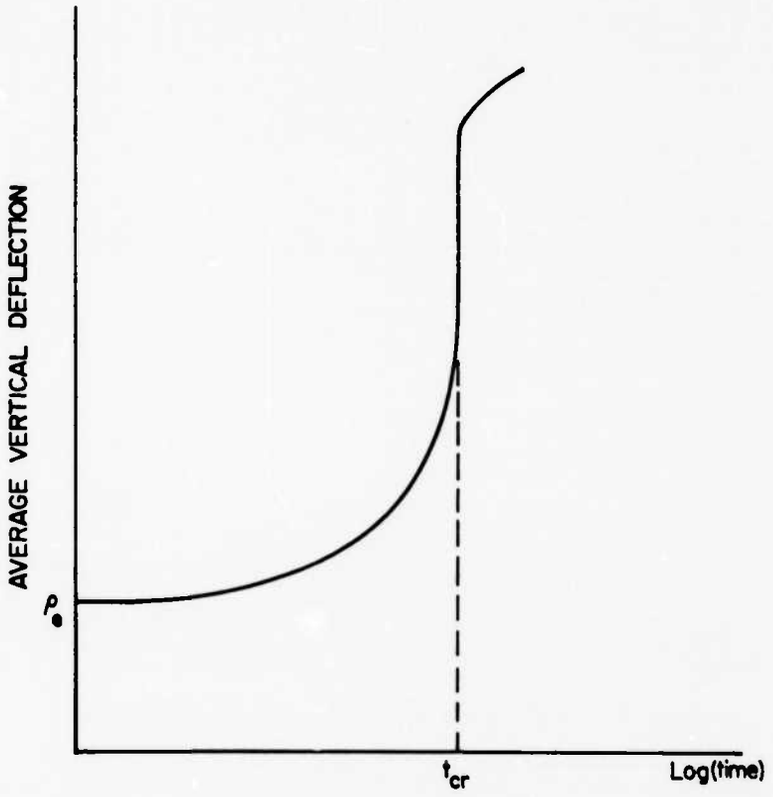

FIG. 2. Average Vertical Deflection of Clamped Shallow Spherical Shells

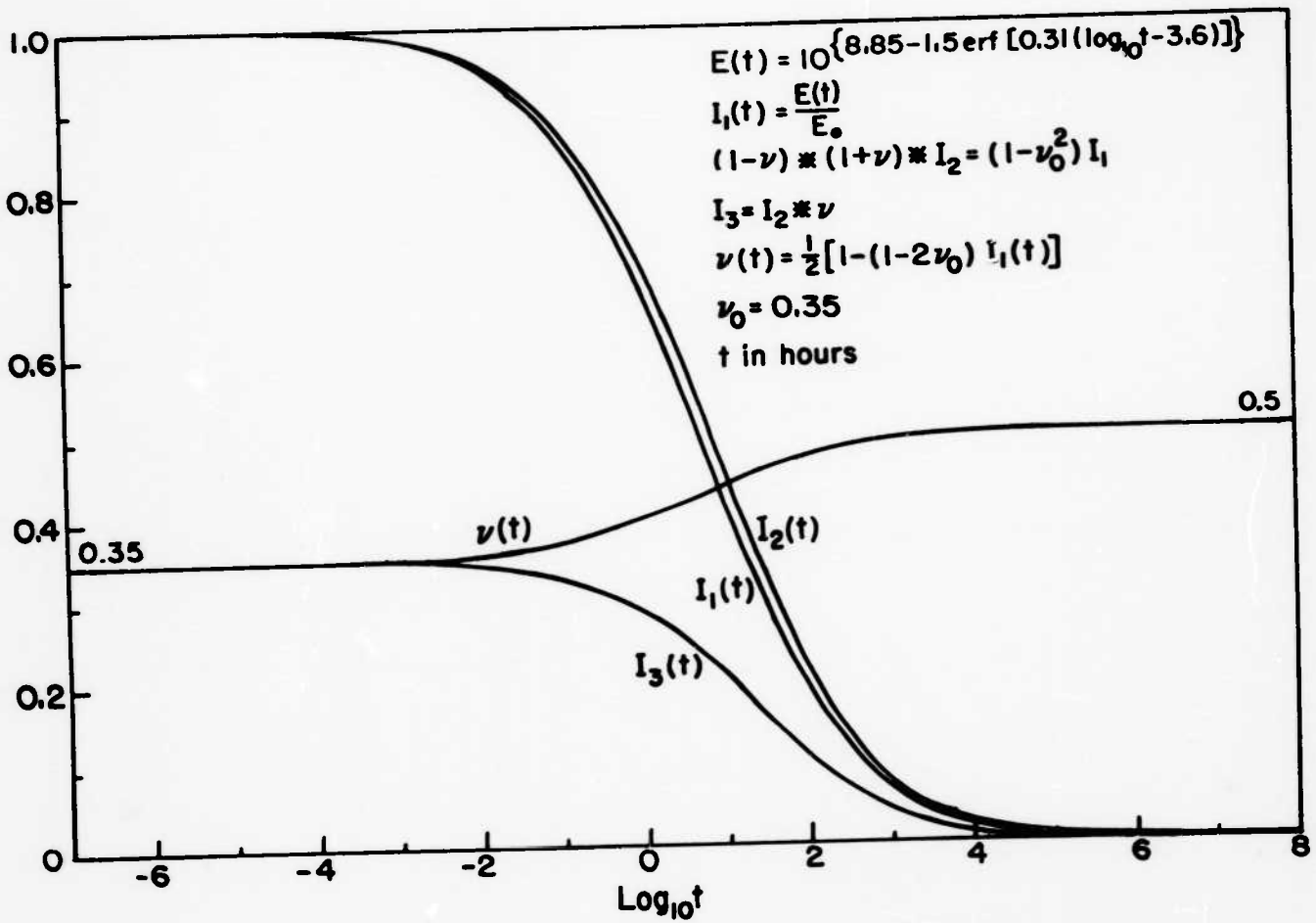

FIG. 3. Viscoelastic Shell Constances for Polymethyl Methacrylate

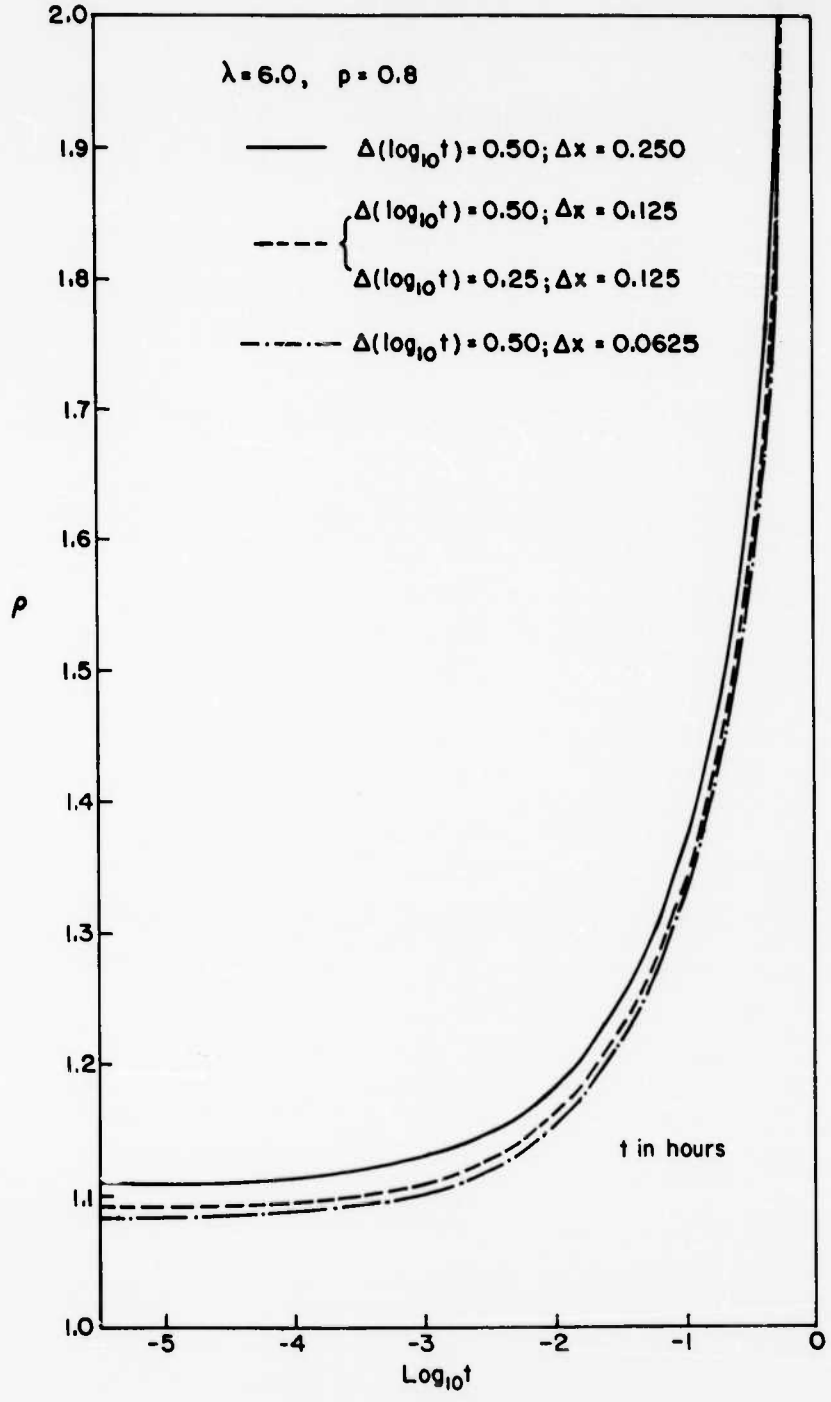

FIG. 4. Comparison of Average Vertical Deflections for Different Time Intervals and Different Space Intervals

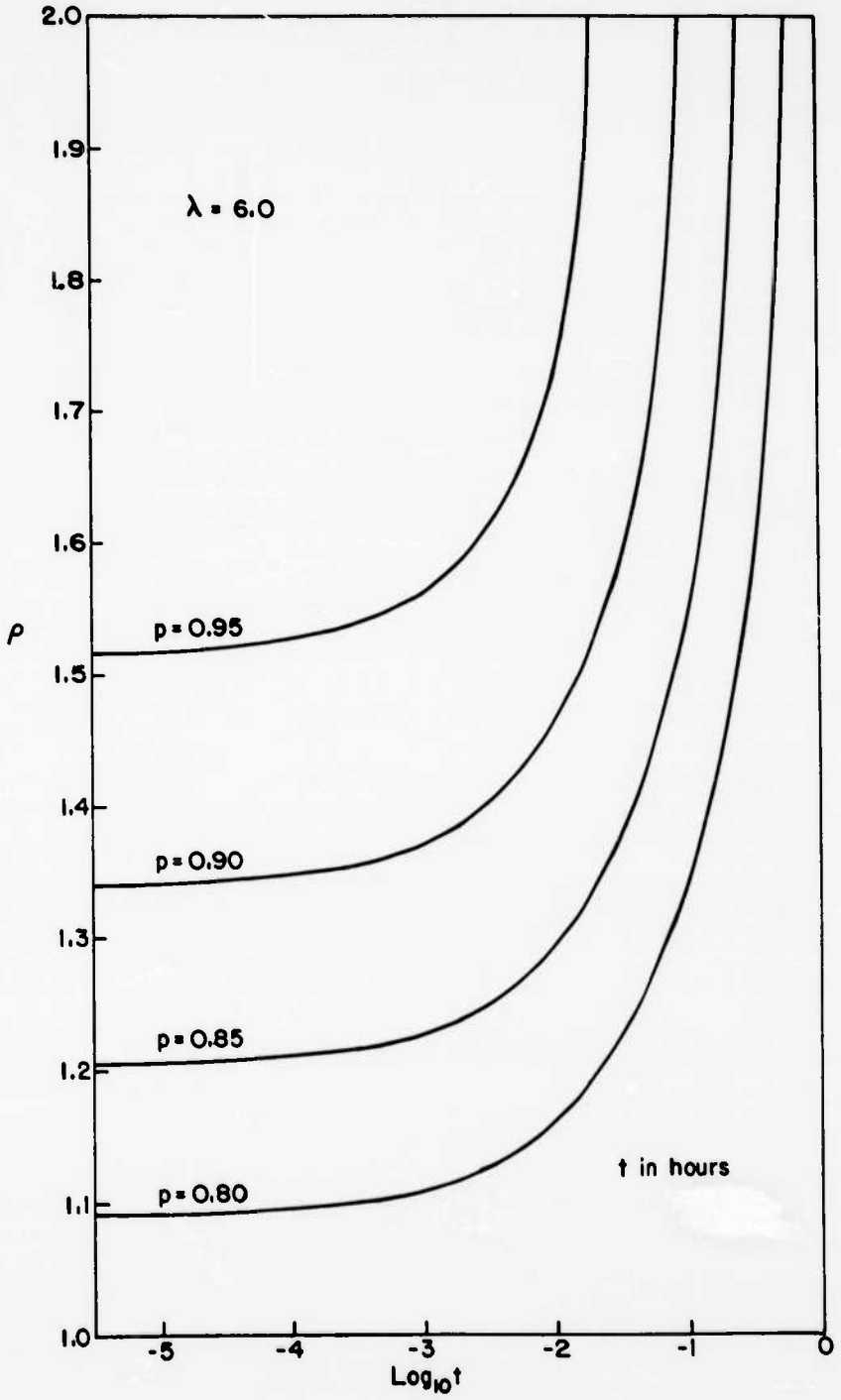

FIG. 5. Average Vertical Deflections for $\lambda = 6$

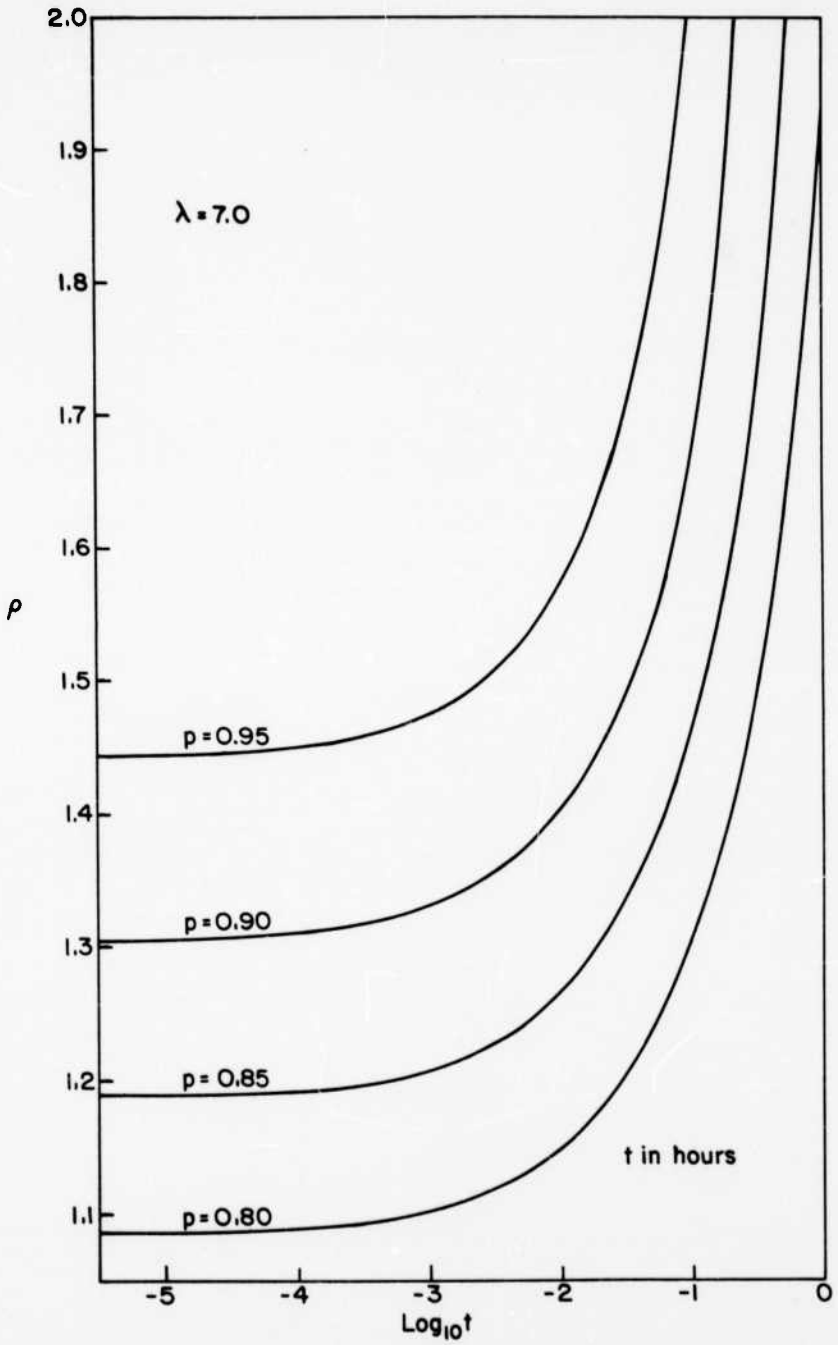

FIG. 6. Average Vertical Deflections for $\lambda = 7$

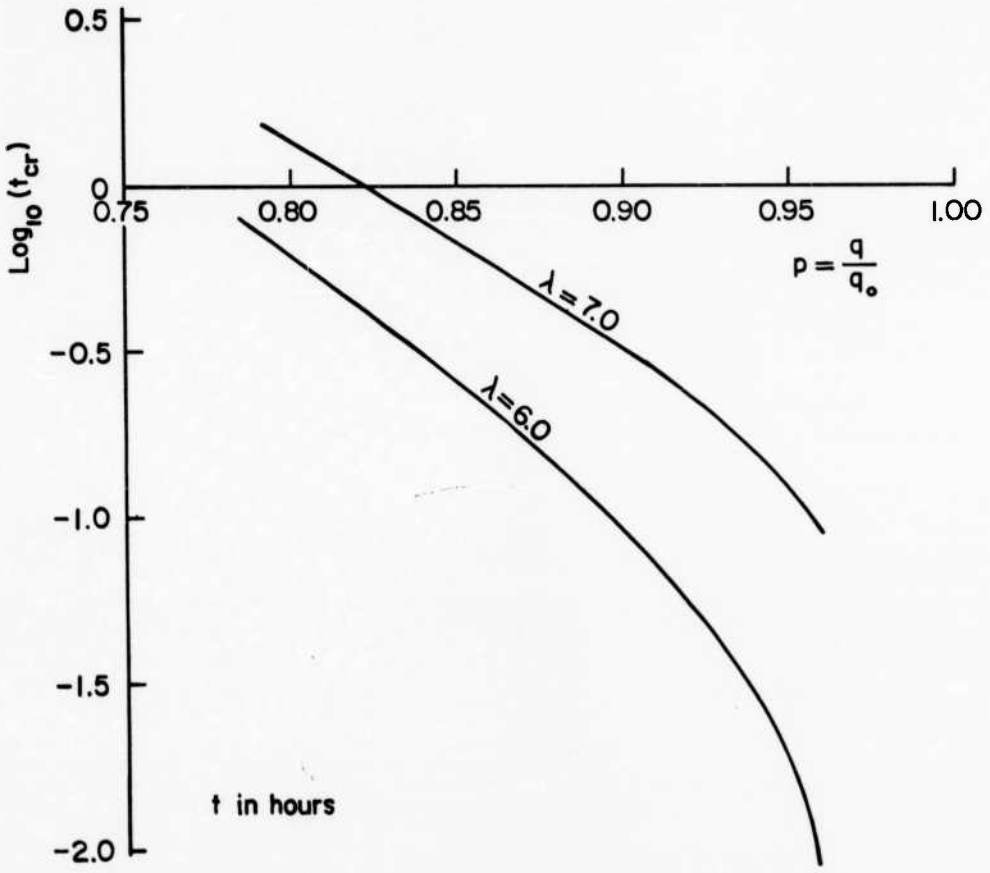

FIG. 7. Critical Times for $\lambda = 6$ and $\lambda = 7$

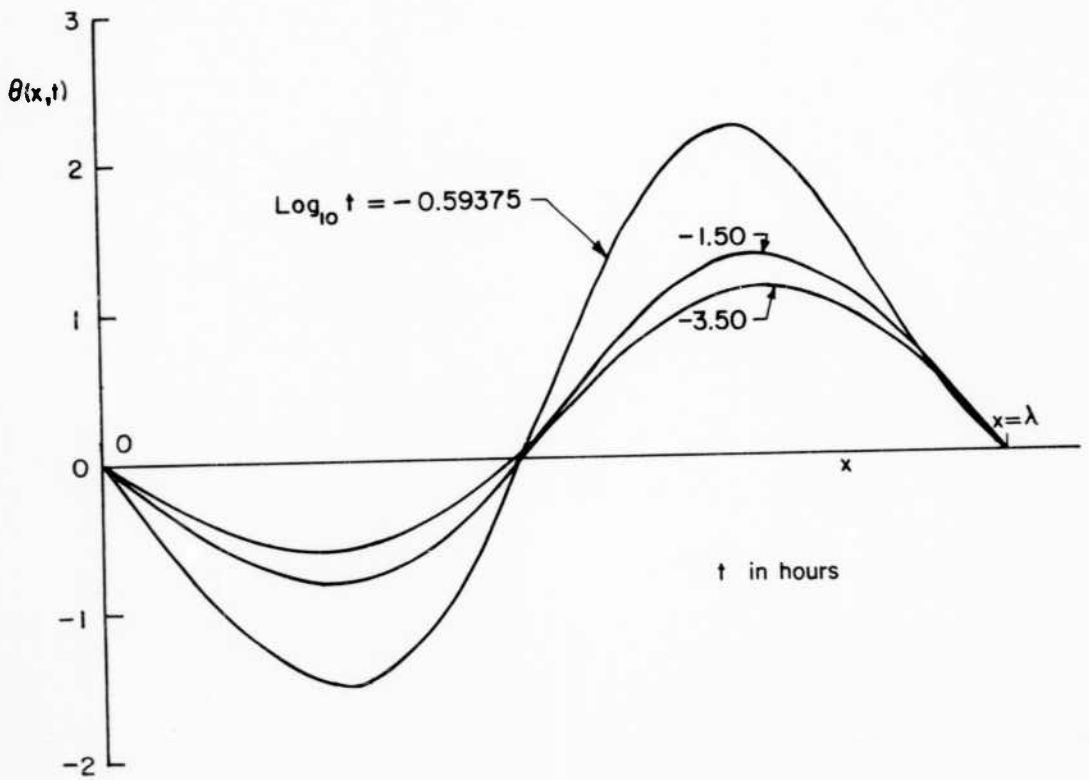

FIG. 8. θ Distributions for $\lambda = 6$ and $p = 0.85$

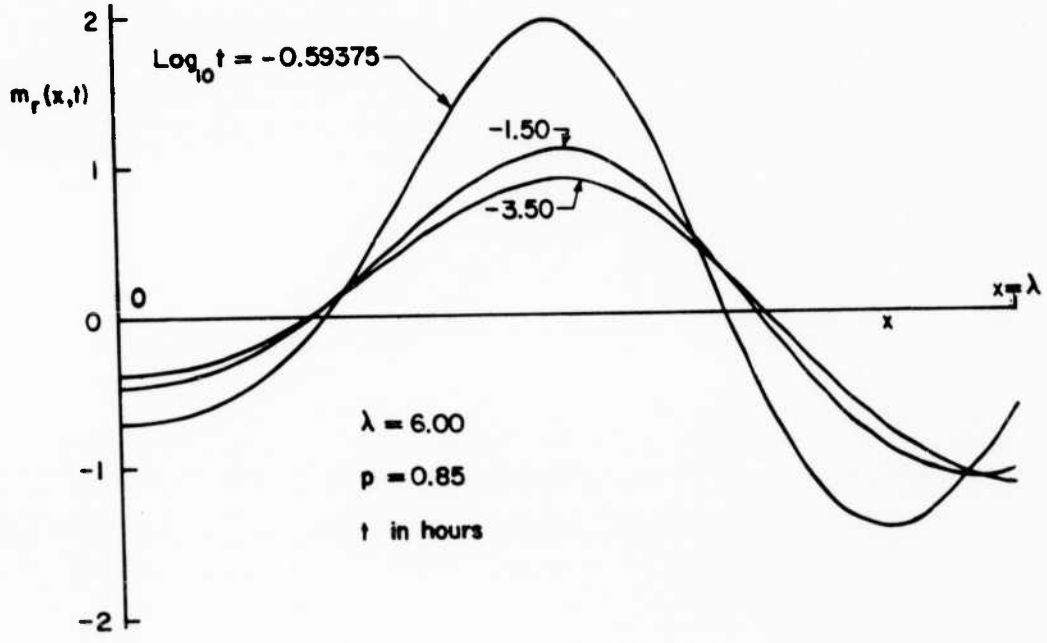

FIG. 9. m_r Distributions for $\lambda = 6$ and $p = 0.85$

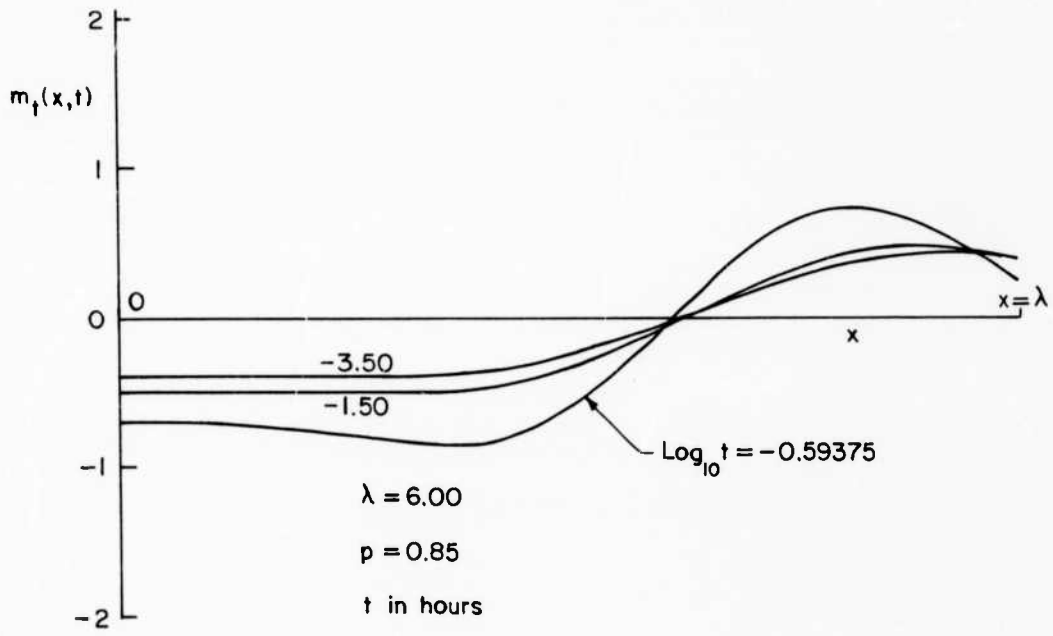

FIG. 10. m_t Distributions for $\lambda = 6$ and $p = 0.85$

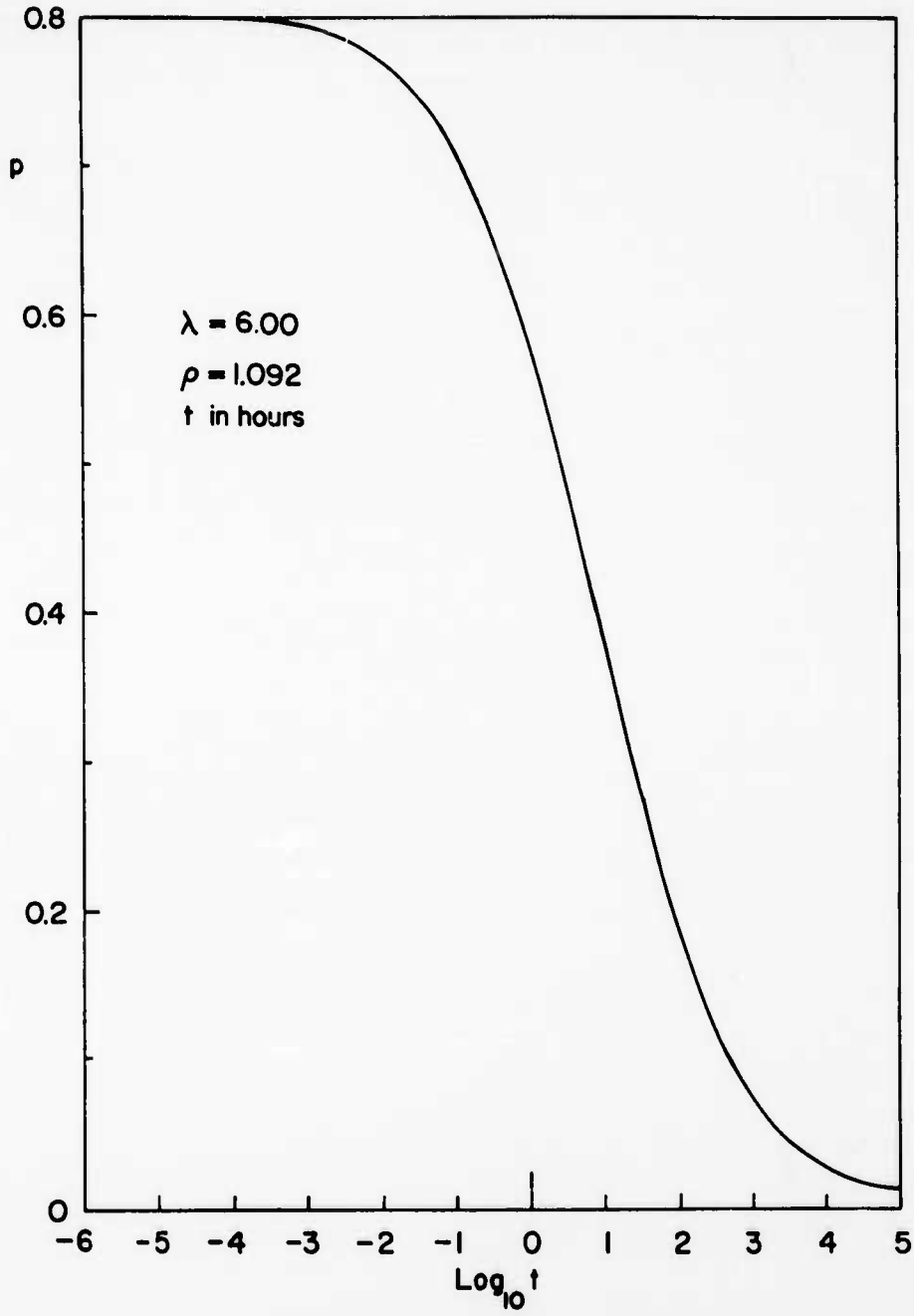

FIG. 11. Relaxation of External Pressure When ρ is Specified.

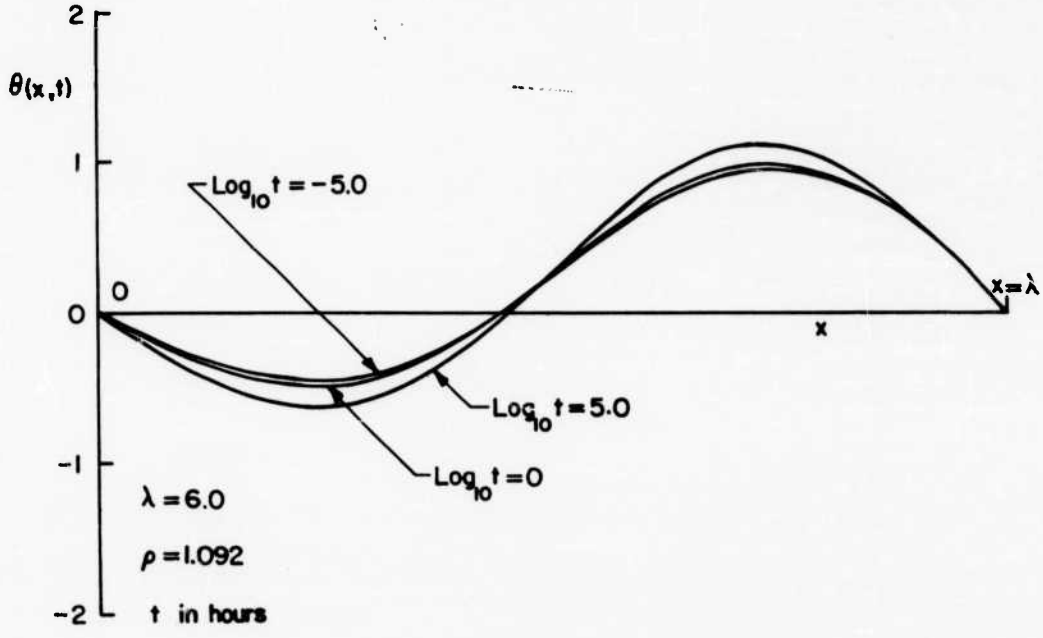

FIG. 12. θ Distributions When ρ is Specified

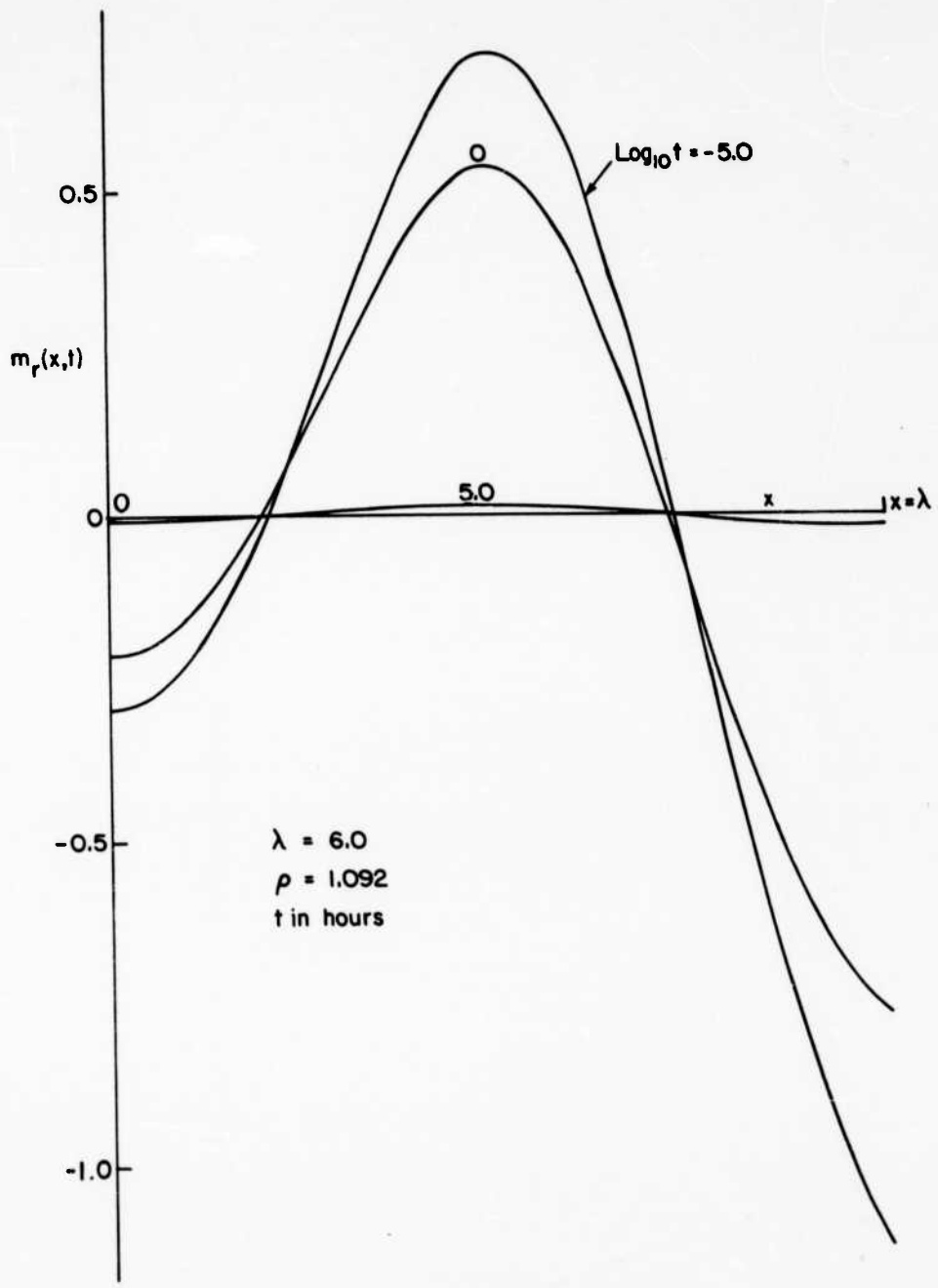

FIG. 13. m_r Distributions When ρ is Specified

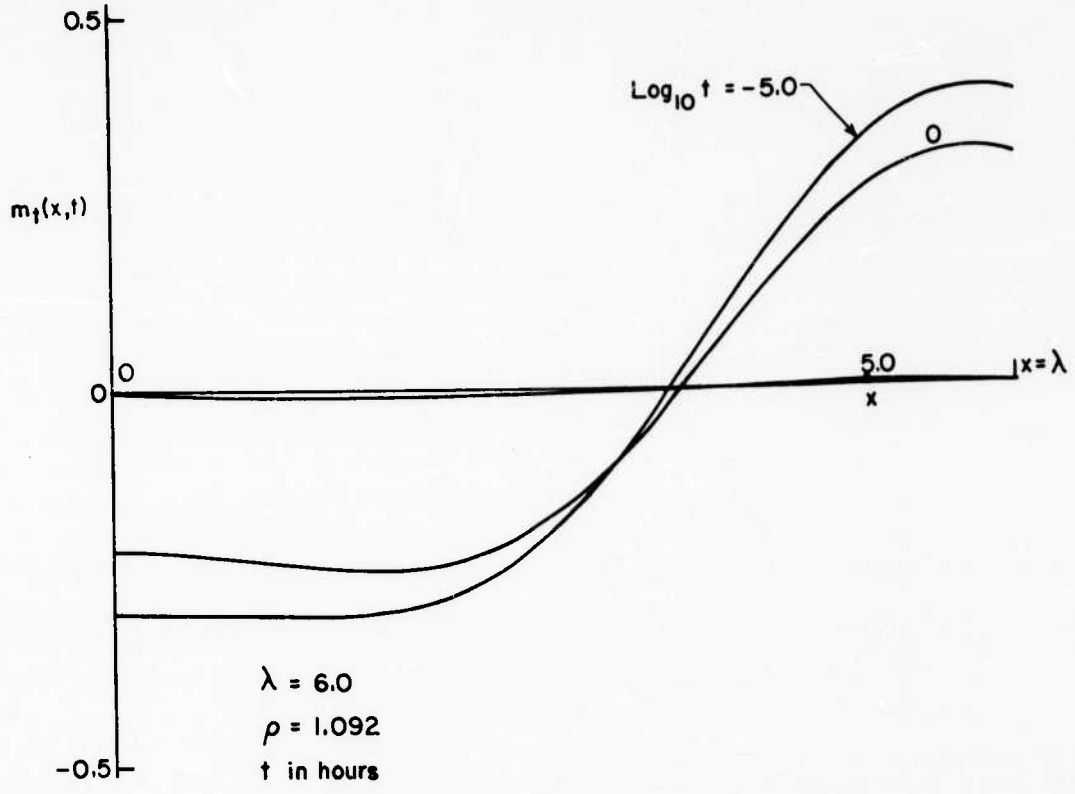

FIG. 14. m_t Distributions When ρ is Specified